

# Model-based reconstruction of real-world fractal complex networks

Kordian Makulski, Mateusz Samsel, Michał Lepek, Agata Fronczak, Piotr Fronczak  
Faculty of Physics, Warsaw University of Technology, Koszykowa 75, Warsaw, PL-00-662, Poland  
(Dated: February 7, 2025)

This paper presents a versatile model for generating fractal complex networks that closely mirror the properties of real-world systems. By combining features of reverse renormalization and evolving network models, the proposed approach introduces several tunable parameters, offering exceptional flexibility in capturing the diverse topologies and scaling behaviors found in both natural and man-made networks. The model effectively replicates their key characteristics such as fractal dimensions, power-law degree distributions, and densities. Unlike traditional deterministic models, it incorporates stochasticity into the network growth process, overcoming limitations like discontinuities in degree distributions and rigid size constraints. The model's applicability is demonstrated through its ability to reproduce the structural features of real-world fractal networks, including the Internet, the World Wide Web, and co-authorship networks.

## INTRODUCTION

Fractal complex networks constitute a remarkable and intriguing class of complex networks that are distinguished by their self-similarity and power-law scaling properties across a wide range of scales [1–4]. These networks are not confined to theoretical constructs; they appear ubiquitously in both natural and man-made systems. Examples include biological networks, such as neuronal or vascular systems, where structural and functional organization often reflects fractal-like patterns [5], the World Wide Web, which demonstrates hierarchical and scale-free properties [1], and social networks, where communities often form self-similar clusters [6–8].

Modeling fractal networks is crucial to discovering the fundamental principles that govern the organization and evolution of these systems. Fractal network models provide a framework for studying processes such as information flow [9], robustness [10], and spreading dynamics [11], which are deeply influenced by the network's structure. By accurately modeling fractal networks, we can design more efficient and resilient infrastructures, predict behaviors in natural and engineered systems, and better understand the interplay between topology and function in such environments.

The primary feature distinguishing fractal networks from non-fractal networks is the power-law relationship between the network size  $N$  and its diameter  $L$  in the form:  $N \sim L^{d_B}$ , where the exponent  $d_B$  is referred to as the fractal dimension [4]. Non-fractal networks are characterized rather by an exponential relationship,  $N \sim e^L$ , and, due to short distances between nodes, are commonly known as *small-world* networks.

When defining complex fractal networks, one must proceed carefully, as there exist fractal networks that are not complex (e.g., road networks [12] or random graph models at the percolation threshold [1]). Likewise, there are complex networks that, like fractal networks, exhibit scale-invariance in their degree distribution (such as the famous Barabási-Albert (BA) evolving network model

[13]), but are not structurally self-similar under renormalization and their size grows exponentially with the diameter [1].

The aforementioned renormalization is a process in which nodes in the network are grouped into "boxes" based on a predefined distance, and these groups are treated as super-nodes in a newly constructed network. Remarkably, fractal networks preserve their statistical properties through such successive renormalizations, demonstrating self-similarity that can be quantitatively analyzed [1, 9]. For example, the degree distribution  $P(k)$  as well as the distribution of the normalized masses of boxes  $P(\mu) \sim \mu^\delta$  retain their power-law character both before and after renormalization [8]. This property sets them apart from other types of networks, such as small-world networks, which lack such explicit self-similarity under renormalization.

To avoid misunderstandings, in this work, we define complex fractal networks as those that possess a well-defined fractal dimension  $d_B$ , a power-law distributions  $P(k)$  and  $P(\mu)$ , and are structurally self-similar under renormalization.

Since in real-world networks it is generally infeasible to directly analyze the relationship between their size and diameter (which remain unchanged), the most common method for determining the fractal dimension  $d_B$  is through the box-covering procedure [15, 16]. This method yields a relationship between the number of boxes  $N_B$  required to cover the network and the size (diameter) of each box  $l_B$ , expressed as:

$$N_B(l_B) \propto l_B^{-d_B}. \quad (1)$$

Although the first models of fractal networks appeared at the beginning of this century, they remain relatively scarce and are limited in their properties. Despite the inevitable randomness inherent in the evolution of real fractal networks, most existing models are deterministic [2, 17–20]. In a few exceptions, such as models based on random walks [21, 22] construction method appears

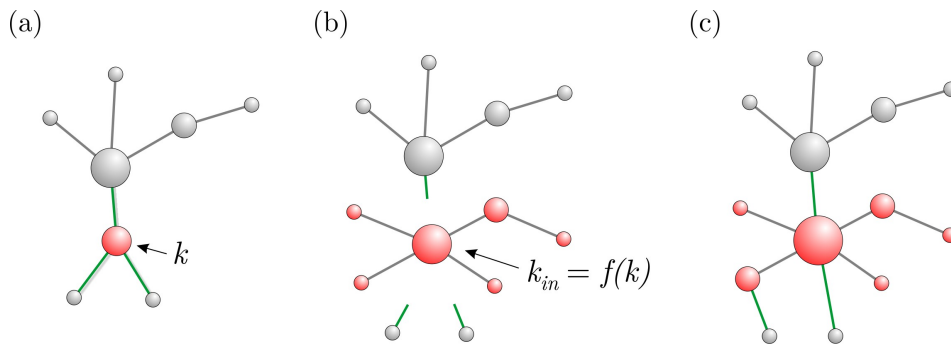


FIG. 1. The network growth process in the model. (a) A node is randomly selected. (b) A new subnetwork is generated in place of the node selected in (a). (c) Preferential reconnection of external links takes place.

somewhat artificial and rather difficult to justify with the underlying processes occurring in real-world networks.

The deterministic models are usually based on the procedure of reverse renormalization, in which in place of a single node (or edge) representing a given unit at a higher scale, a more complex structure is introduced that better reflects the details of the original nodes or edges. The models of this class, such as the Song-Havlin-Makse (SHM) model [2] and the  $(u, v)$ -flower model [23], offer analytical tractability and allow precise verification of statistical methods. However, they also introduce artificial discontinuities, such as abrupt jumps in the degree distribution and restrictions on network size, which cannot be adjusted freely. The SHM model generates scale-free fractals with a tree-like structure, where the fractal dimension  $d_B$  and the degree distribution exponent  $\gamma$  are interdependent. On the other hand, the  $(u, v)$ -flower model replaces edges with subnetworks of fixed paths, controlled by parameters  $u$  and  $v$ , enabling different fractal configurations.

While these deterministic models are mathematically elegant, their limitations reduce their applicability to modeling real-world systems, which often exhibit randomness and lack strict structural constraints. Recently, two models have been proposed that generalize SHM and  $(u, v)$ -flower models and aim to overcome their limitations [24, 25]. The first model [24] introduced randomness into the SHM framework, which, unlike earlier attempts, preserves the fractal nature of the generated network. In the second model [25], a network is iteratively constructed by replacing each edge in the previous generation's network with a smaller graph, called a generator. The choice of generators allows for independent control over the scale-free property, fractality, and other structural characteristics of the generated network. Additionally, the introduction of stochasticity makes this model a promising direction for the further development of fractal network models. However, it replicates the issues of models based on reverse renormalization, such as the discontinuity in the distributions  $P(k)$  and  $P(\mu)$ , and the

strictly defined network sizes resulting from the number of renormalization steps taken.

In this paper, we propose a new model of fractal networks that lies at the intersection of reverse renormalization-based models and evolving network models. Unlike deterministic alternatives, our approach introduces randomness at every stage of network construction, eliminating artificial discontinuities. The proposed model allows for flexible adjustment of key network parameters, including size, fractal dimension, degree distribution exponent  $\gamma$ , and edge density. Moreover, it can produce networks with a high clustering coefficient, making it suitable for replicating real-world networks. We present several examples where our model faithfully captures the key characteristics of real-world networks.

The remainder of this paper is organized as follows: Section 2 introduces the construction procedure of the model. Section 3 presents real-world datasets used for comparisons. Section 4 discusses the main results, highlighting the model's ability to replicate key features of real-world networks. Finally, Section 5 concludes the study.

## MODEL

1. The network growth process starts with two nodes connected by a single edge.
2. At each step, a node  $i$  of degree  $k_i$  is randomly selected from the existing network. It becomes the starting point for the subprocess that generates a new subnet.
  - (a) The subnet grows based on linear preferential attachment, following a generalized Barabási-Albert (BA) model:
    - Each newly added node has an initial attractiveness  $A$  and connects with  $m$  existing nodes in the same subnet.

Network	$N$	$\langle k \rangle$	$d_B$	$\gamma$	$\delta$	$A$	$m$	$\alpha$	$k_{top}$
AS-Caida	77,339	12.7	5.2	2.1	2.2	0.15	6.35	1.6	30,000
WWW Google	855,802	10.0	3.7	2.5	2.5	0.3	5	2.5	1,000
DBLP	8,805	2.6	2.2	2.8	2.8	0.5	1.3	0.9	38

TABLE I. Values of the parameters of the fractal networks used in the study. In the table,  $N$  is the number of nodes in the analyzed network,  $\langle k \rangle$  is the average node degree,  $d$  corresponds to the diameter of the network, and  $d_B$  is the fractal dimension obtained using our FNB algorithm and the Song's GC algorithm. Numbers in brackets give theoretical values, if known. Note low diameters of the protein interaction and autonomous system (AS) networks. For those networks, obtaining finite fractal dimension  $d_B$  was not possible within the GC approach.

- The probability of connecting a new edge to an existing node  $j$  is proportional to  $A+k'_j$ , where  $k'_j$  is the internal (within the subnet) degree of node  $j$  (thus, at the beginning of the subprocess, the initial node  $i$  has  $k'_i = 0$ ).
  - (b) The growth of the subnet stops when the most well-connected node node within the subnet (i.e. a local hub) reaches the maximum degree  $k'_{max} = f(k_i)$ , where  $f$  is some increasing function controlling the scaling of the degree of the initial node  $i$ .
  - (c) After the subnet's growth is complete,  $k_i$  edges, which originally connected the initial node to the rest of the network, are reassigned with the same preference to nodes within the newly created subnet.
3. The process stops when the size of the network reaches  $N$ .

Although this model exhibits traces of reverse renormalization, it remains local at each time step, limited to a single node (this can be called *asynchronous reverse renormalization*). Therefore, this model is closer to the class of evolving networks, where the network evolution occurs continuously on two timescales: the selection of a source node on a longer timescale and the evolution of a subnet on a shorter timescale. The network growth process is schematically illustrated in Fig. 1.

In this model, the parameter  $A$  represents the initial attractiveness of newly added nodes and plays a crucial role in shaping the topology of the generated subnetwork. It is inspired by the generalized BA model introduced by Dorogovtsev et al. [26], where depending on initial attractiveness, the scaling exponent  $\gamma$  of the node degree distribution takes values from 2 to  $\infty$ . Although Dorogovtsev et al. derived an exact relationship between  $A$  and the scaling exponent  $\gamma$ , in our model this relationship is approximate. Specifically, for  $A = 1$ , we obtain a scaling exponent  $\gamma \approx 3$ , and as  $A$  decreases, the value of  $\gamma$  also decreases. This allows us to model networks with  $\gamma$  values between 2 and 3, which are the most commonly observed in real-world networks.

The function  $f(k)$ , which defines the maximum degree  $k'_{max}$  of the subnetwork created in place of a node with degree  $k$ , plays a role similar to the inverse renormalization procedure. Specifically, while renormalization typically aggregates fine-grained details into larger, simplified structures,  $f(k)$  effectively reverses this process by generating more detailed, fine-scale structures (a subnetwork) from a single, coarse-grained element (the original node). This allows the model to reintroduce complexity at smaller scales, reflecting the hierarchical and multi-scale nature of real-world networks.

The function  $f(k)$  must satisfy certain requirements. First, it must enable the emergence of nodes with increasingly higher degrees in the network, so that by the end of the network growth process, a heterogeneous (preferably power-law) degree distribution can be established. Second, it must limit the creation of excessively large subnetworks, which, being part of the universality class of the BA model, are non-fractal and could overshadow the fractal profile of the entire network. Therefore, there must be a certain upper limit for the degree,  $k'_{max} = k_{top}$ , returned by this function, where  $k_{top}$  represents the highest degree of a node in the entire network. In our study, we adopted a function of the form:

$$f(k) = \frac{k^\alpha}{1 + \frac{k^\alpha}{k_{top}^\alpha}}, \quad (2)$$

The shape of this function for parameters  $\alpha = 1.5$  and  $k_{top} = 1000$  is shown in Fig. 2.

This function can be understood as a map that transforms a node with degree  $k$  into another node (and its surrounding subnetwork) with degree  $f(k)$ . If this new node is transformed again, the process can be schematically expressed as the composition of two functions,  $f(f(k))$ . In Fig. 2, we have illustrated a longer sequence of such mappings using orange lines.

Notice that as the parameter  $\alpha$  increases, the number of such mappings decreases. When this number becomes too small, the system ceases to exhibit self-similarity in-depth because the number of renormalization steps (nested subnetworks) that can be performed on the network is directly tied to the number of mappings through the function  $f$ .

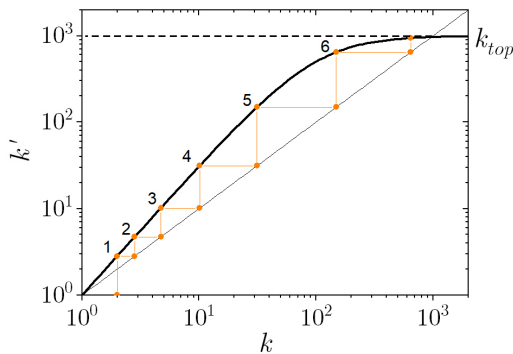


FIG. 2. An example plot of the function  $f(k)$  (thick line). Subsequent mappings of this function are highlighted in orange, illustrating how nodes with increasingly higher degrees emerge in the network with each successive generation of subnets.

On the other hand, the parameter  $\alpha$  cannot be too small. A value less than one would prevent the network from generating nodes with higher degrees. Although a value slightly greater than one corresponds to a very large number of mappings, it is important to remember that with each mapping, the number of nodes in the network increases (as a new subnetwork emerges). Consequently, it is possible for the network to reach its intended size before nodes with high degrees (close to  $k_{top}$ ) appear.

Through trial-and-error, we determined an intermediate value of the parameter,  $\alpha = 1.5$ , which allows for multiple levels of nested subnetworks while ensuring that sufficiently high node degrees appear in the network.

In summary, the model is defined by five parameters:  $N$ ,  $m$ ,  $A$ ,  $\alpha$ , and  $k_{top}$ , which correspond to the size, density, exponent  $\gamma$ , self-similarity, and the maximum degree of the nodes in the generated network, respectively.

## DATASETS

To demonstrate the usefulness of the proposed model in reflecting real-world networks, we analyzed the key characteristics of three different networks that have distinct fractal exponents:

- Internet at the level of autonomous systems: In context of the Internet, an autonomous system (AS) is a collection of associated Internet Protocol (IP) prefixes with a clearly defined routing policy. It governs how the AS exchanges routing information with other autonomous systems. An AS can be thought of as a connected group of IP networks which are managed by a single administrative entity, e.g. a university, government, commercial organization or other type of internet service provider. The AS network ('AS-caida') analyzed by us contains 77.3 k nodes, a graph derived by

CAIDA [27] from a set of RouteViews [28] BGP table snapshots from 1 November 2024. We obtained this network from public repository at [29].

- WWW (Google web graph): The web subset analysed consists of 856 k web pages that are linked if there is a URL link from one page to another [30]. The dataset is publicly available in several network repositories (e.g. [31]).
- DBLP coauthorship network: DBLP is a digital library of article records published in computer science [32, 33]. In this study, similarly as in Refs. [7, 8], we use the 12th version of the dataset (DBLP-Citation-network V12; released April 2020, which contains information on approximately 4.9 M articles published mostly during the last 20 years). We ourselves processed the raw DBLP data into the form of coauthorship network, from which we extracted the network backbone by imposing a threshold on the minimum number of joint papers ( $\geq 20$ ) two scientists should have. This procedure significantly reduced the size of the studied network (from 2.9 M nodes and 12.5 M links to 8.8 k nodes and 11.4 k edges), but thanks to it the network became naturally fractal.

The main characteristics of these networks as well as the used parameters of the model are presented in Tab.

## RESULTS

In Fig. 3, we present heat maps of the fractal dimension  $d_B$  (Fig. 3a) and the degree distribution exponent  $\gamma$  (Fig. 3b) as functions of the parameters  $A$  and  $k_{top}$ . The results were obtained for  $N = 10^6$  and  $m = 1$ . As shown, the model allows for a wide range of desired values for these exponents:  $d_B$  ranges from 2 to 5, and  $\gamma$  ranges from 2 to 3, which aligns with the range of  $\gamma$  values observed in most real-world networks with power-law degree distributions.

The parameter  $A$ , similar to its role in the original Dorogovtsev model, allows for tuning the desired degree distribution, while the parameter  $k_{top}$  primarily influences the fractal properties of the generated network.

It is worth noting that creating such a map for networks of this size was made possible by a recently developed box-covering algorithm, which enables highly efficient computation of fractal dimensions, even for very large networks [34]. In opposite to standard box-covering methods, the algorithm calculates fractal dimension of complex networks by covering them with boxes whose sizes are not equal. In this approach, hubs (i.e. nodes of degree larger than some threshold) are selected as the initial seeds for each box, and nodes are then assigned to

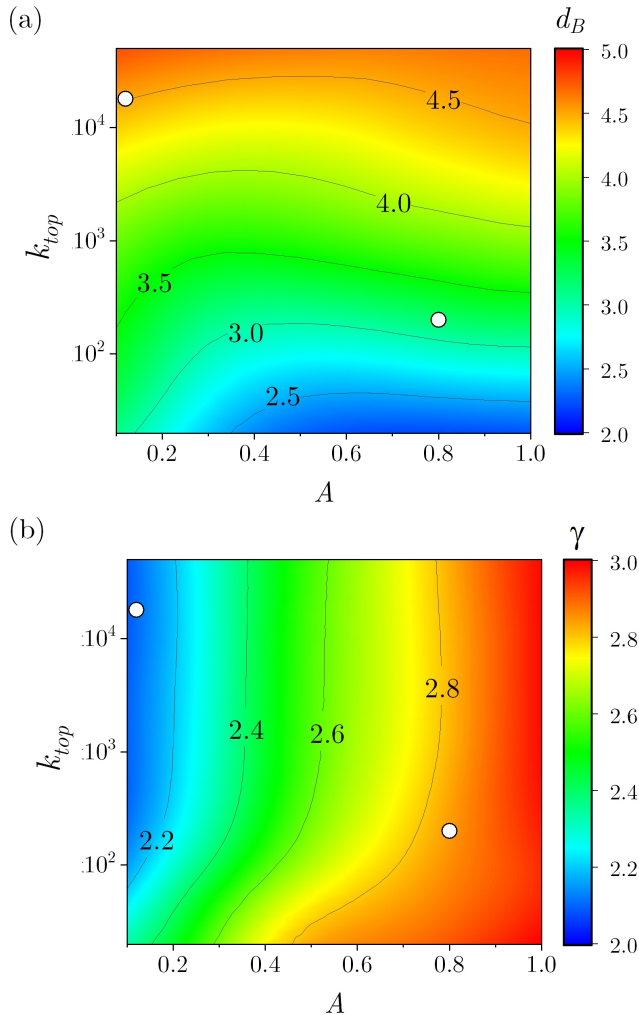


FIG. 3. Heat maps illustrating how the fractal dimension  $d_B$  (a) and the degree distribution exponent  $\gamma$  (b) depend on two model parameters:  $A$  and  $k_{top}$ . The white circles indicate the parameters used to generate the networks shown in Fig. 4. The plots present averaged results over 20 network generations, each with  $N = 10^6$ ,  $m = 1$ , and  $\alpha = 1.5$ .

their nearest hubs, regardless of the actual distance. By covering the network with boxes that vary in hub number  $N_B$  (controlled by threshold value of a node degree) one can generate different sets of boxes and then, calculating for each set an average box size,  $\langle l_B \rangle$ , one can estimate the necessary coverage  $N_B(\langle l_B \rangle)$ . As has been shown in [34], this approach offers greater flexibility and accuracy in analyzing fractal networks.

In Fig. 4, we show both analyzed characteristics,  $N_B(\langle l_B \rangle)$  and  $P(k)$ , for two selected sets of parameters from the map in Fig. 3 (marked with white circles on the heat map).

Fig. 5 illustrates how the exponents  $d_B$  and  $\gamma$  analyzed in our study vary with network size. As shown, the degree distribution exponent  $\gamma$  remains relatively stable,

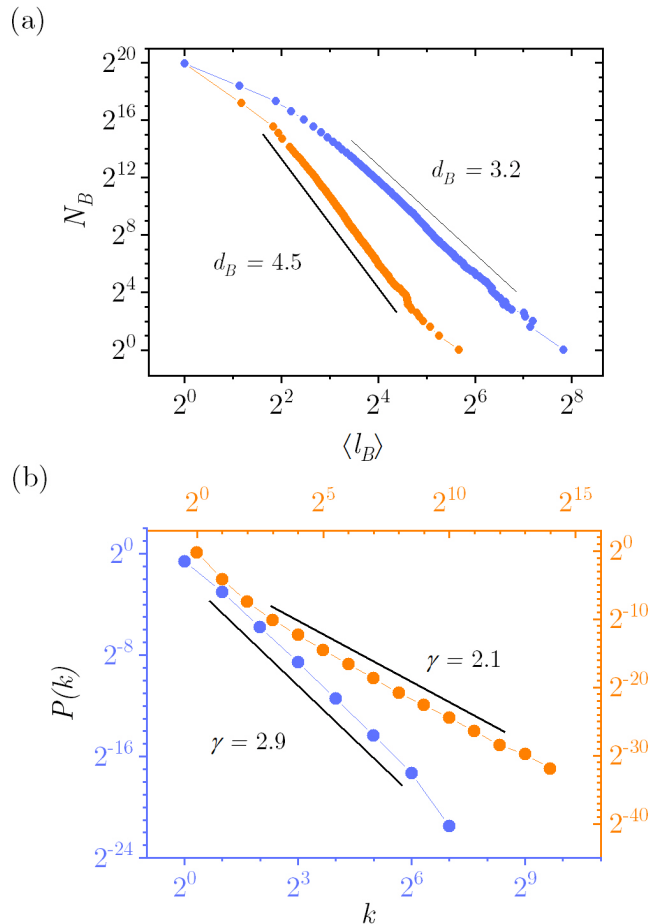


FIG. 4. Macroscopic characteristics of generated fractal complex networks: (a) the number of boxes  $N_B$  needed to cover the considered networks as a function of the mean diameter  $\langle l_B \rangle$  of the box, (b) the node degree distributions  $P(k)$ . The parameters used are shown in Fig. 3 as white circles.

whereas the fractal dimension  $d_B$  increases significantly with network size, eventually stabilizing for  $N > 10^6$ . This effect is particularly pronounced for the curve corresponding to higher values of  $d_B$ .

Therefore, the heat map in Fig. 3, which was generated for  $N = 10^6$ , may differ slightly for networks of other sizes. However, the general pattern—i.e., the dependence of  $d_B$  and  $\gamma$  on the model parameters  $A$  and  $k_{top}$ —will remain unchanged.

Achieving the desired values of  $d_B$  and  $\gamma$  may require an iterative approach to fine-tune the control parameters. The sequence of steps we propose is as follows: First, the parameters  $N$  and  $m$  can be determined based on the properties of the real-world network - its size and the average node degree, respectively. Next, by adjusting the parameter  $A$ , the desired value of the exponent  $\gamma$  can be achieved. Finally, by modifying the parameter  $k_{top}$ , the appropriate value of the fractal dimension  $d_B$  can be obtained.

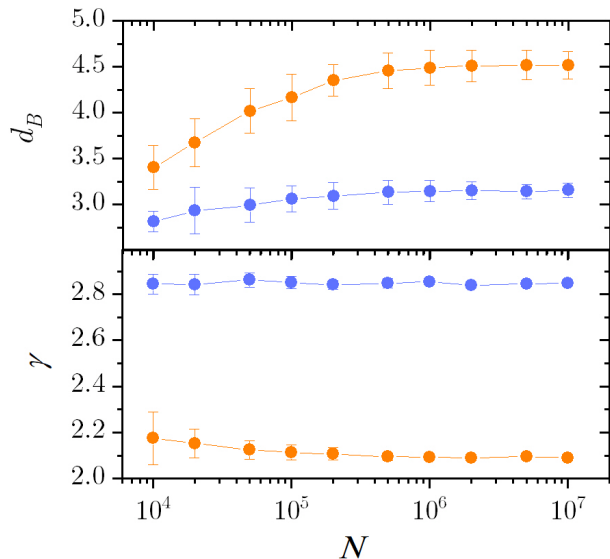


FIG. 5. The dependence of macroscopic parameters  $d_B$  and  $\gamma$  on the size  $N$  of the generated network. The parameters correspond to the white points in Fig. 3, and the values are averaged over 20 network generations.

Finally, we aim to demonstrate the usefulness of the proposed model in capturing the properties of real-world networks. In Fig. 6, we compare the outputs of the model with the corresponding real-world datasets for three distinct networks. Notably, in addition to the relationships  $N_B(l_B)$  and  $P(k)$ , the distribution of normalized box masses  $P(\mu)$ , shown in Fig. 6 on panels (c), (f), and (i), also exhibits strong agreement between the model and its real-world counterpart. By normalized box masses, we mean the number of nodes within individual boxes used to cover the network. These numbers are divided by the average box mass obtained for a given covering. In Figure 6, the box covering was performed for boxes whose hub degrees are larger than 4.

Please note that, to accurately reflect the characteristics of real-world networks, we had to adjust also the parameter  $\alpha$ . In some networks (see especially panels (a) and (g) in Fig. 6), power-law scaling only emerges at intermediate values of  $\langle l_B \rangle$ , while at smaller values, the behavior is more characteristic of an exponential relationship. Adjusting parameter  $\alpha$  allows for fine-tuning the behavior of  $N_B$  for small values of  $\langle l_B \rangle$ . It is also worth noting that the networks presented are not trees and have a relatively high average degree (see Tab. ), yet our model performs exceptionally well in fitting the data.

The clustering coefficient values obtained for the networks shown in Fig. 6 are roughly half of those observed in real-world networks (e.g., in the WWW network,  $C = 0.51$ , while in its model,  $C = 0.29$ ). This value could be significantly increased by modifying the

model—for example, by allowing a new node, when attaching to  $m$  existing nodes within its subnet, to preferentially connect to nodes that are already its neighbors, thereby forming a larger number of triangles, as in the model of Holme and Kim [35]. However, in this study, we prefer to keep the model in its basic form.

## SUMMARY AND CONCLUSIONS

The proposed model offers a comprehensive framework for generating fractal networks with tunable characteristics. It is defined by five key parameters that provide flexibility in modeling a wide range of network structures, making the model applicable to various real-world systems.

The model's iterative construction process, driven by reverse renormalization principles, highlights its capability to generate complex networks with localized growth dynamics. By limiting the evolution to a single node at each step, the model emulates realistic scenarios where local interactions drive global network properties. This approach also bridges the gap between static fractal network models and dynamic, evolving systems.

Future work could explore extensions of the model, such as incorporating weighted edges, dynamic rewiring, or multilayer structures, to further enhance its applicability and relevance.

## CODE

In the supplementary materials, we have provided Python code for generating networks according to the presented model, as well as tools for analyzing the obtained network, including the mentioned box-covering algorithm. The code was written with a focus on efficiency at the expense of readability. This allows for the generation and analysis of large networks within a reasonable time (e.g., generating a network with  $N = 10^6$  on a standard laptop takes approximately 15 seconds, while the box-covering process adds another 60 seconds).

## ACKNOWLEDGMENTS

Research was funded by Warsaw University of Technology within the Excellence Initiative: Research University (IDUB) programme.

---

[1] C. Song, S. Havlin, H.A. Makse, Self-similarity of complex networks, *Nature* **433** (2005) 392-395.

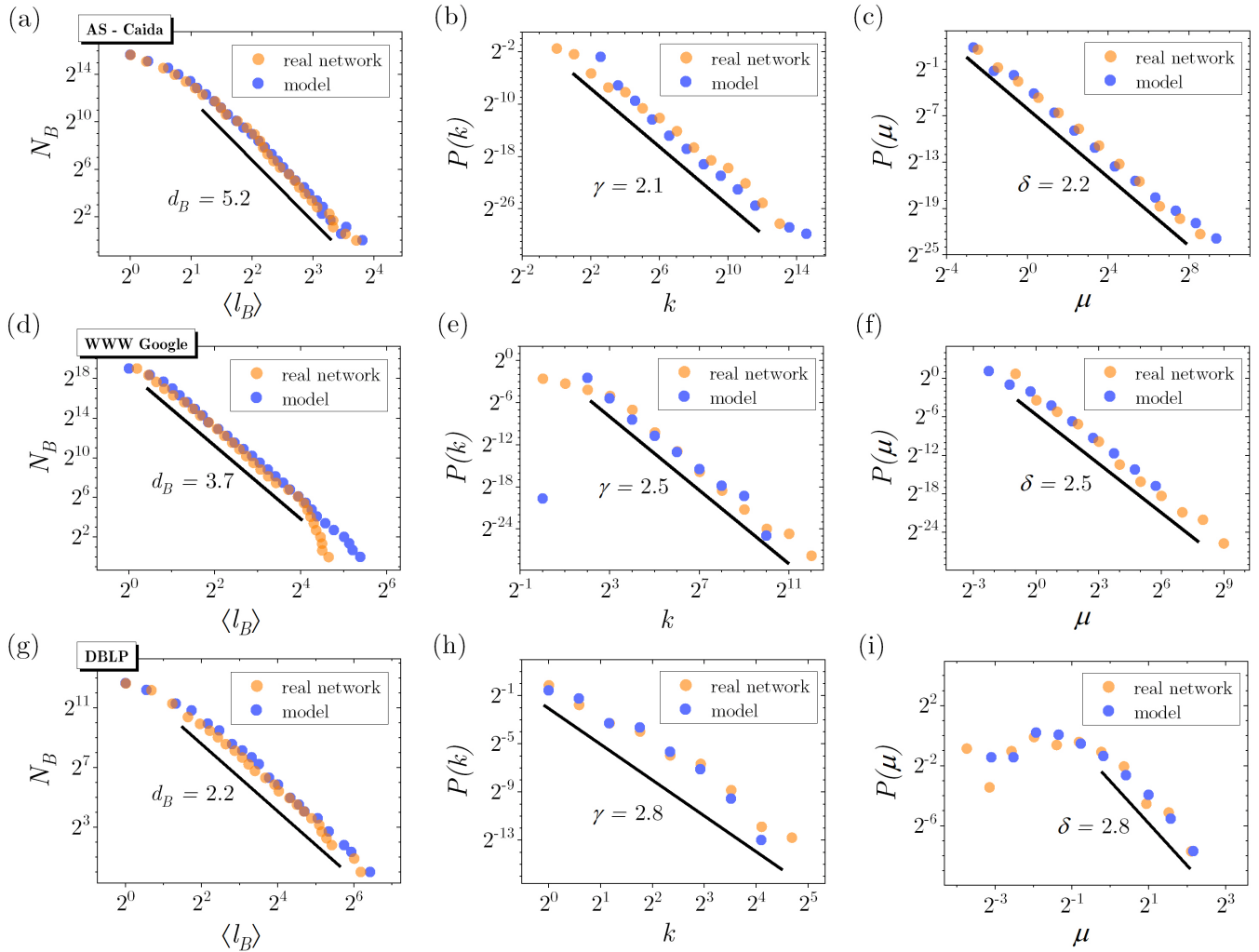


FIG. 6. A comparison of the characteristics of three real-world networks (orange points) with those of networks generated using the proposed model (blue points). The graphs placed in the same row refer to the same network (i.e. Internet, WWW and DBLP, respectively). In particular, the following graphs show: (a,d,g) – a log-log plot of  $N_B$  versus  $\langle l_B \rangle$  revealing the fractal nature of the network according to Eq. (1), (b,e,h) – the node degree distribution  $P(k)$ , (c,f,i) – the normalized mass box distribution  $P(\mu)$ . The parameters of the fitted models as well as characteristics of real networks are gathered in Tab. .

- [2] C. Song, S. Havlin, H.A. Makse, Origins of fractality in the growth of complex networks, *Nat. Phys.* **2** (2006) 275-281.
- [3] T. Wen, K.H. Cheong, The fractal dimension of complex networks: a review, *Inf. Fusion* **73** (2021) 87-102.
- [4] E. Rosenberg, *Fractal Dimensions of Networks*, Springer (2020).
- [5] L.K. Gallos, H.A. Makse, M. Sigman, A small world of weak ties provides optimal global integration of self-similar modules in functional brain networks, *Proc. Natl. Acad. Sci. U.S.A.* **109** (2012) 2825-2830.
- [6] L.K. Gallos, F.Q. Potiguar, J.S. Andrade Jr, H.A. Makse, IMDB Network Revisited: Unveiling Fractal and Modular Properties from a Typical Small-World Network. *PLOS ONE* 8(6): e66443 (2013)
- [7] A. Fronczak, M.J. Mrowinski, P. Fronczak, Scientific success from the perspective of the strength of weak ties, *Sci. Rep.* **12** (2022) 5074.
- [8] A. Fronczak, P. Fronczak, M.J. Samsel, et al., Scaling theory of fractal complex networks, *Sci. Rep.* **14** (2024) 9079.
- [9] H.D. Rozenfeld, C. Song, H.A. Makse, Small-world to fractal transition in complex networks: A renormalization group approach, *Phys. Rev. Lett.* **104** (2010) 025701.
- [10] Wu Y., Chen Z., Yao K., Zhao X., Chen Y., On the correlation between fractal dimension and robustness of complex networks, *Fractals* 27 (04) (2019).
- [11] A. Deppman, E.O. Andrade-Ii, Emergency of Tsallis statistics in fractal networks. *PLoS One*. 2021 Sep 29;16(9):e0257855.
- [12] H. Zhang, P. Gao, T. Lan, C. Liu, Exploring the Structural Fractality of Urban Road Networks by Different Representations. *The Professional Geographer*, 73(2), 348–362 (2021).
- [13] A.L. Barabasi, R. Albert. Emergence of scaling in random networks. *Science* 286(5439):509-12 (1999).

- [14] H.D. Rozenfeld, L.K. Gallos, C. Song, H.A. Makse, Fractal and transfractal scale-free networks, in: R. Meyers, (eds) *Encyclopedia of Complexity and Systems Science*. Springer, New York, NY (2009).
- [15] C. Song, L.K. Gallos, S. Havlin, H.A. Makse, How to calculate the fractal dimension of a complex network: the box covering algorithm, *J. Stat. Mech.* (2007) P03006.
- [16] P.T. Kovács, M. Nagy, R. Molontay, Comparative analysis of box-covering algorithms for fractal networks, *Appl. Netw. Sci.* **6** (2021) 73.
- [17] C. Zeng and M. Zhou, Small-world and scale-free properties of fractal networks modeled on n-dimensional sierpinski pyramid, *Fractals*, vol. 25, p. 1750057 (2017).
- [18] C. Zeng, Y. Xue, and Y. Huang, Fractal networks with sturmian structure, *Physica A*, vol. 574, p. 125977 (2021).
- [19] A. Le, F. Gao, L. Xi, and S. Yin, Complex networks modeled on the sierpinski gasket, *Physica A*, vol. 436, pp. 646–657 (2015).
- [20] L. Huang and Y. Zheng, Asymptotic formula on APL of fractal evolving networks generated by durer pentagon, *Chaos, Solitons Fractals*, vol. 167, p. 113042 (2023).
- [21] P. Chehminiak, Emergence of fractal scale-free networks from stochastic evolution on the cayley tree, *Physics Letters A*, vol. 377, p. 2846–2850 (2013).
- [22] N. Ikeda, Fractal networks induced by movements of random walkers on a tree graph, *Physica A*, vol. 537, p. 122743 (2020).
- [23] H.D. Rozenfeld, S. Havlin, D. Ben-Avraham, Fractal and transfractal recursive scale-free nets, *New. J. Phys.* **9** (2007) 175.
- [24] E. Zakar-Polyak, M. Nagy, and R. Molontay, Investigating the origins of fractality based on two novel fractal network models, in *Complex Networks XIII* (D. Pacheco, A. S. Teixeira, H. Barbosa, R. Menezes, and G. Manigioni, eds.), (Cham), pp. 43–54, Springer International Publishing, 2022.
- [25] K. Yakubo and Y. Fujiki, A general model of hierarchical fractal scale-free networks, *PLOS ONE*, vol. 17, p. e0264589, (2022).
- [26] S.N. Dorogovtsev, J.F.F. Mendes, and A.N. Samukhin, Structure of growing networks with preferential linking, *Phys. Rev. Lett.* **85**, 4633 (2000).
- [27] Center for Applied Internet Data Analysis, <https://www.caida.org/catalog/datasets/as-relationships/>, accessed: 2024-10-04.
- [28] University of Oregon RouteViews Project, <https://www.routeviews.org/>, accessed: 2024-10-04.
- [29] Stanford Large Network Dataset Collection, <https://snap.stanford.edu/data/as-Caida.html>, accessed: 2024-10-04.
- [30] J. Leskovec, K.J. Lang, A. Dasgupta, M.W. Mahoney, Community structure in large networks: Natural cluster sizes and the absence of large well-defined clusters, *Internet Mathematics* **6** (2009) 29-123.
- [31] R.A. Rossi, N.K. Ahmed, The network data repository with interactive graph analytics and visualization, *Proc. AAAI Conf. Artificial. Intell.*, **29**(1) (2015), <https://networkrepository.com>.
- [32] J. Tang, A.C.M. Fong, B. Wang, J. Zhang, A unified probabilistic framework for name disambiguation in digital library, *IEEE Trans. Knowl. Data Eng.* **24** (2012) 975-987.
- [33] DBLP Citation Network Dataset, <https://www.aminer.org/citation>, accessed: 2022-08-30.
- [34] M. Lepek, K. Makulski, A. Fronczak, P. Fronczak, Beyond traditional box-covering: Determining the fractal dimension of complex networks using a fixed number of boxes of flexible diameter, arXiv:2501.16030.
- [35] P. Holme and B. J. Kim, Growing scale-free networks with tunable clustering, *Phys. Rev. E*, **65**, 026107 (2002).